PHYSICAL REVIEW B VOLUME 27, NUMBER 2 15 JANUARY 1983

Electronic and lattice contributions to the thermal conductivity of graphite intercalation compounds

J-P. Issi and J. Heremans
Université Catholique de Louvain, Laboratoire de Physico-Chimie et de Physique de l'Etat Solide, Place Croix du Sud, 1, B-1348 Louvain-la-Neuve, Belgium

M. S. Dresselhaus
Center for Materials Science and Engineering and Department of Electrical Engineering and Computer Science, Massachusetts Institute of Technology, Cambridge, Massachusetts 02139
(Received 26 July 1982)

The stage and temperature dependences of the in-plane thermal conductivity of graphite-$FeCl_3$ acceptor intercalation compounds are reported and analyzed, as well as the temperature dependence of a stage-5 potassium donor compound. The measured thermal conductivity is tentatively separated into an electronic contribution, which is dominant at low temperatures, and a lattice contribution, which is dominant around room temperature. Quantitative information is provided about lattice defects which are introduced by intercalation and scatter both electrons and phonons. Below room temperature the in-plane lattice thermal conductivity is reduced by about an order of magnitude relative to pristine graphite due to an equivalent decrease in boundary scattering length and, to a lesser extent, to point defect scattering. Electron and phonon scattering is only weakly stage dependent. Data for the c-axis thermal conductivity of a stage-2 $FeCl_3$ and a stage-5 potassium compound are also presented and discussed.

I. INTRODUCTION

Graphite is an anisotropic layered material in which the in-plane covalent binding forces are much larger than the interplanar van der Waals—type binding forces. In spite of very high in-plane electrical mobilities ($\sim 1\ m^2 V^{-1} sec^{-1}$ at 300 K, compared to $\sim 3\times 10^{-3}\ m^2 V^{-1} sec^{-1}$ for metals), graphite has a relatively poor conductivity ($2.5\times 10^6\ \Omega^{-1} m^{-1}$ at 300 K), because of its small density of electrons and holes ($\sim 2\times 10^{25}\ m^{-3}$ at 300 K). The insertion between the graphite layers of atomic or molecular layers of extrinsic species called the intercalant, leads to the formation of either donor or acceptor graphite intercalation compounds (GIC's) depending on the intercalant. The intercalate layers are periodically arranged in the matrix of the graphite layers, with the number of graphite layers between adjacent intercalation layers denoting the stage index of the GIC. A comprehensive review on the properties of GIC's has recently been presented.[1]

The charge transfer between intercalant and graphite layers results in an increased density of highly mobile carriers, which confers to GIC's electrical conductivities comparable to those of the best metallic conductors ($\sim 6\times 10^7\ \Omega^{-1} m^{-1}$). Because of their promise as synthetic materials of high electrical conductivity, GIC's have in the last few years attracted a great deal of attention.[1] However, it was only very recently that exploratory thermal conductivity studies were performed on acceptor[2,3] and donor[3,4] GIC's. These investigations gave new insights into the thermal-conduction phenomena in two-dimensional solids as well as into the transport properties of the GIC's.

In the previous work,[2–5] it was shown that for both donor and acceptor compounds, intercalation leads to a decrease of the in-plane lattice thermal conductivity and to an increase of the electronic contribution relative to pristine graphite. In the c-axis direction, the thermal conductivity was attributed entirely to the lattice. Also, contrary to the case of the electrical conductivity, the anisotropy of the thermal conductivity was found comparable to that of pristine graphite around room temperature. At low temperatures it was found that heat is entirely carried by phonons in one direction (c axis) and electrons in another direction (in-plane).

The conduction of heat in crystalline solids below room temperature is mainly due to two distinct mechanisms: the lattice conductivity κ_L and the contribution from the charge carriers κ_E. If both mechanisms are operative, then the total thermal

conductivity is given by

$$\kappa = \kappa_E + \kappa_L \ . \tag{1}$$

It was shown that, contrary to pristine graphite where only κ_L is important for the entire temperature range $3 < T < 300$ K, both κ_E and κ_L are effective in a GIC below room temperature. In the liquid-helium range, the thermal conductivity was found to vary linearly with temperature, suggesting that κ_E is dominant. This was further confirmed experimentally by applying a high magnetic field to separate the electronic and lattice contributions.[6]

In its simplest form, the lattice thermal conductivity is given by the well-known Debye formula

$$\kappa_L = \tfrac{1}{3} C_v v \lambda \ , \tag{2}$$

where C_v is the lattice specific heat at constant volume, v is the group velocity of phonons (the velocity of sound), and λ the phonon mean free path.

The electronic contribution to the thermal conductivity is directly related to the electrical conductivity σ through the Wiedemann-Franz law (WFL)

$$\kappa_E = L \sigma T \ , \tag{3}$$

where the coefficient L takes the value of the Lorenz number $L_0 = 2.44 \times 10^{-8}\ \mathrm{V^2 K^{-2}}$ for a free electron system. The WFL is only valid when the scattering of electrons is elastic. This is the case at low temperatures for pure metals, where the dominant scattering mechanism for the electrons is by static defects, and around and above the Debye temperature, where large-angle electron-phonon scattering is dominant.[7]

Preliminary data reported for a donor and an acceptor GIC have shown that thermal-conductivity measurements provide valuable information concerning electrical and thermal transport properties. At high temperatures where lattice thermal conductivity dominates, these measurements provide information about phonon scattering mechanisms, while at lower temperature where electronic conductivity dominates, they yield quantitative information on electronic scattering processes.[5] In the present work we extend these ideas in a more quantitative form and present as well some new experimental results. The present work also emphasizes the stage dependence of the lattice and electronic thermal conductivities.

II. EXPERIMENTAL

A. Samples

All samples were prepared from the highly oriented pyrolytic graphite (HOPG) host material. Typical sample dimensions were $20 \times 4 \times 0.5\ \mathrm{mm^3}$ for in-plane measurements and $4 \times 4 \times 1\ \mathrm{mm^3}$ for c-axis measurements. A standard two-zone furnace was used to prepare the $FeCl_3$ compounds, and the stage was controlled by adjusting the temperature difference between the graphite and the $FeCl_3$ powder.[8] Well-staged samples were synthesized using a gas pressure of ~ 500 Torr Cl_2. Thermal transport measurements were made on graphite-$FeCl_3$ samples of stages 2, 3, 4*, and 6 prepared in this way. With regard to thermal transport measurements on donor compounds, a sample of stage-5 potassium GIC was selected, since its Fermi surface had already been studied extensively.[9] It was also shown that for graphite-potassium compounds of stage $n > 4$ the desorption rate under ambient conditions is slow,[10] and this observation was used to simplify the sample handling procedure. All samples were stored in ampoules and were always handled in a controlled dry-nitrogen atmosphere, free from water vapor and oxygen, until the sample was mounted in the sample chamber of the cryostat. The samples were mounted as quickly as possible and the sample chamber was then evacuated to $\sim 10^{-5}$ Torr.

After intercalation, all samples were characterized by (00l) x-ray diffractograms to determine the stage index, stage fidelity, and c-axis repeat distance I_c. After performing the thermal-conductivity measurements, x-ray diffractograms were taken again to ensure that thermal cycling from liquid helium to room temperature did not affect the staging. It was also verified on all samples that thermal cycling did not affect the residual resistivity and that the thermal-conductivity results were reproducible from run to run. All samples studied in this work were well staged, except for the stage-4 $FeCl_3$ sample, which showed admixtures of stages 5 and 6 and is therefore labeled as $n = 4^*$.

B. Sample holders and measuring techniques

Static thermal-conductivity measurements were performed using a heater and sink method. Since the in-plane thermal conductivity is about 2 orders of magnitude greater than that along the c axis, a different sample holder had to be designed for the two geometries. Specifically, the geometry of the sample should be different according to whether a good or a poor thermal conductor is being measured.[11] The l/A ratio (where l is the length of the sample and A its cross section) should be large for a good conductor and small for a poor conductor, consistent with the dimensions of the available sam-

ples, since the larger dimensions are in-plane. Experimental details for the thermal conductivity measurements as well as the detailed description of the sample holders designed and used for the measurements are given elsewhere.[12] In all cases electrical contacts to the samples were made with a tiny drop of silver paint. With and without silver paint no detectable change was found in the low-temperature electronic thermal conductivity (which provides direct information on the residual electrical resistivity, see Sec. IV A), indicating that the silver paint did not alter the electronic properties of our samples.

The experimental accuracy for the thermal-conductivity measurements depends on the temperature range, sample orientation, and sample dimensions. The highest accuracies are achieved for in-plane measurements using samples of larger cross sections in the lowest-temperature range, where the estimated error is $\sim 1\%$; the accuracy for the same samples is $\sim 3\%$ around room temperature. The maximum estimated error is for c-axis samples around room temperature, where it may reach $\sim 5\%$. In addition, due to the uncertainties in estimating the distance between the thermometers, the absolute magnitude of κ_a in the curves for the in-plane thermal conductivity might have to be multiplied as a whole by a factor ranging from 0.95 to 1.05. Thus, the thermal-conductivity data are more accurate with regard to temperature variation than with regard to absolute magnitudes.

Usually, when thermal-conductivity measurements are performed on electrical conductors, it is of paramount importance to be able to measure the electrical resistivity on the same sample. The separation of lattice and electronic contributions is then facilitated to a great extent. However, this type of separation is not easy to perform for the in-plane thermal conductivity for GIC's because of the high anisotropy of the electrical conductivity, which for the case of acceptor compounds necessitates the use of contactless measurement techniques.[13]

III. RESULTS

A. The in-plane thermal conductivity

In Fig. 1 we present the temperature variation of the thermal in-plane conductivity κ_a in graphite-$FeCl_3$ acceptor compounds (stages 2, 3, 4*, and 6) and in a stage-5 graphite-potassium donor compound for the temperature range $2 < T < 300$ K.

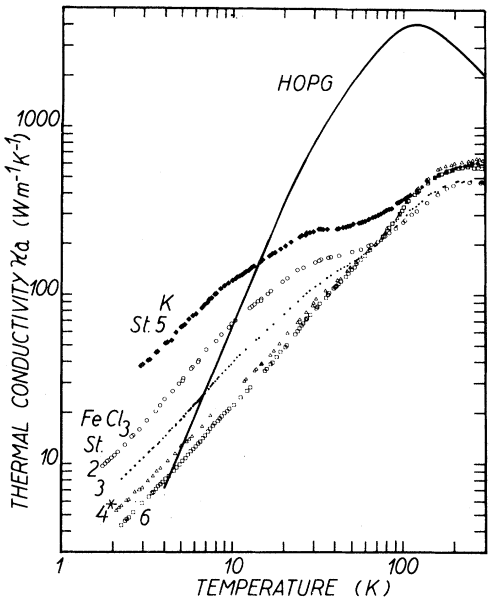

FIG. 1. Temperature variation of the in-plane thermal conductivity κ_a of various graphite intercalation compounds compared to that of pristine HOPG (solid line). Results are presented for pure stages: 2 (open circles), 3 (dark circles), and 6 (open squares), and a mixed 4* stage (open triangles) $FeCl_3$ acceptor GIC. Data for a stage-5 potassium donor intercalation compound are also presented (dark squares).

For comparison we also show thermal-conductivity results for a pristine graphite (HOPG) sample of the same origin as the starting material used in the preparation of our intercalation compounds.[2]

Starting from the lowest temperature, we see that for the stage-2 $FeCl_3$ compound there is a very narrow temperature range $T < 3$ K over which the thermal conductivity κ_a varies linearly with temperature. Above the linear temperature regime, the measured thermal conductivity increases more rapidly with temperature and shows a tendency to level off above 30 K. At higher temperature, the thermal conductivity again increases with temperature to reach, finally, a very broad maximum or plateau. In the stage-3 $FeCl_3$ sample the low-temperature linear behavior extends to a higher temperature (to ~ 10 K) and the sample exhibits at yet higher temperatures approximately the same behavior as the stage-2 sample, except that the departure from linearity at low temperature is less pronounced. The thermal conductivity of the stage-6 sample increases linearly with temperature to ~ 6 K and then increases a little more rapidly than T^1 above ~ 10 K, until κ_a reaches a flat maximum or plateau above ~ 200 K. Note that for the $FeCl_3$ intercalat-

ed samples, the low-temperature thermal conductivity decreases with increasing stage, while at room temperature the situation is qualitatively reversed. For all the graphite-$FeCl_3$ samples that were investigated, the κ_a-vs-T curves cross (reverse in behavior) at the same temperature of ~ 70 K. The temperature dependence of κ_a for the mixed-stage-4* $FeCl_3$ sample appears to follow the trends of the results for the stage 2, 3, and 6 compounds in Fig. 1.

In the case of the stage-5 potassium compound, the thermal conductivity κ_a begins with a linear T^1 law for $2 < T < 20$ K, but then κ_a starts to level off immediately, unlike the $FeCl_3$ compounds. It is only for $T > 60$ K that κ_a for the stage-5 potassium sample again increases and shows a similar functional behavior as that for the $FeCl_3$ acceptor samples. It is also significant to note that at low temperature all GIC samples exhibit a linear T^1 law while highly ordered pristine graphite samples exhibit no linear T dependence down to 3 K.

B. The c-axis thermal conductivity

The temperature dependence of the c-axis thermal conductivity κ_c, which is presented in Fig. 2 for a stage-2 graphite-$FeCl_3$ sample and a stage-5 graphite-K sample, is quite different in magnitude and in functional form than the in-plane component κ_a. First, the c-axis component at low temperature increases roughly as T^2 with increasing temperature, reaches a maximum around ~ 60 K for the stage-2 graphite-$FeCl_3$ sample, then decreases as the temperature is further increased.

Approximately the same behavior is observed in κ_c for a potassium stage-5 compound, except that in this case the maximum in κ_c is near 20 K, and the magnitude of κ_c exceeds that for the stage-2 $FeCl_3$ compound by a factor of ~ 6 at low T. For comparison we also present the temperature variation of the c-axis thermal conductivity for pristine graphite,[14] which also exhibits a T^2 dependence at low temperature $T < 20$ K, and is a factor of between 10 and 10^2 greater than that for the $FeCl_3$ compound over the entire temperature range. Note too, that for the two GIC samples the anisotropy ratio is several hundred at 300 K and around 100 at 2 K.

IV. DISCUSSION OF THE RESULTS

We shall first discuss the results for the in-plane thermal conductivity κ_a in terms of the contributions of the various types of layers present in the intercalation compound. For each type of layer, we consider the principal heat-conduction mechanisms that are effective below room temperature, i.e., electronic and lattice. Then the c-axis thermal conductivity κ_c will be briefly analyzed.

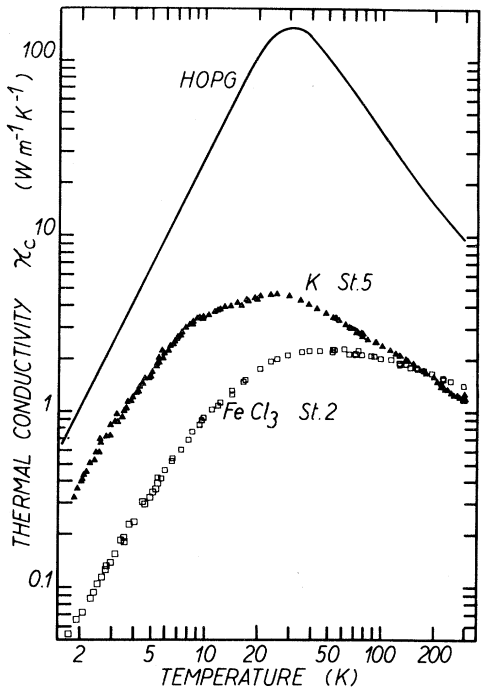

FIG. 2. Temperature variation of the c-axis thermal conductivity κ_c of a stage-2 graphite-$FeCl_3$ acceptor intercalation compound and a stage-5 potassium donor intercalation compound. The curve for pristine HOPG which is taken from Ref. 14 is only given as a rough guide for comparison.

The thermal conductivity κ_a of dilute GIC's has been separated experimentally into electronic and lattice contributions by using high magnetic fields,[6] confirming that at the lowest temperatures κ_a is dominated by pure electronic conduction, as could be expected from the observation of a linear T^1 temperature dependence of κ_a. This electronic conduction is attributed to a large charge-carrier density in the graphite bounding layers; the density of the charge carriers in the graphite interior layers is much lower than in the bounding layers, while the intercalate layers have a very low mobile-carrier density.[1] At higher temperatures, lattice thermal conductivity plays a more important role. Conceivably, in the temperature range between 10 and 30 K, and only for the lowest-stage compounds, might the effect of the intercalant phonons on κ_L be significant.[2-5]

Near room temperature, the thermal conductivity

κ_a is dominated by the lattice contribution of the graphite layers, with a smaller contribution also coming from the charge carriers in the graphite bounding layers. We shall now consider in detail these various contributions.

A. The in-plane electronic thermal conductivity

In discussing the electronic thermal conductivity one should first examine the electrical resistivity data for intercalated graphite. From the temperature dependence of the electrical resistivity $\rho(T)$ of a stage-1 graphite-$FeCl_3$ compound reported by Pendrys *et al.*[15] we see that $\rho(T)$ qualitatively follows the behavior of typical metals, where the total measured electrical resistivity ρ is the sum of a temperature-independent residual contribution ρ_r and a temperature-dependent intrinsic term ρ_i,

$$\rho=\rho_r+\rho_i \ . \tag{4}$$

For typical acceptor compounds the ratio of the room-temperature (300-K) resistivity to that at liquid-helium temperature (4.2 K), [i.e., the residual resistivity ratio (RRR)], is less than 10.[1,15] This can be compared to RRR values of several hundred, or even thousands for pure metals. The situation is quite different for low-stage donor compounds[16–18] where for some samples the RRR (120 for RbC_8 and 218 for KC_8) is comparable to that of pure metals. In this connection, it is of interest to note that the RRR value for *dilute* donor intercalation compounds may be more like that of graphite which is typically ~ 10 for HOPG samples.[19] However, it should be noted that in pristine graphite the carrier density is temperature dependent in contrast to GIC's.[20]

In fact, one should compare residual mobility ratios (RMR) rather than residual resistivity ratios (RRR) for semimetals, which have temperature-dependent carrier densities below room temperature. For these materials the RRR does not have the same meaning as for ordinary metals and GIC's. In the latter materials the RRR is used as a criterion of sample purity and crystalline perfection and in fact also reflects the RMR for the two temperatures considered, 4.2 and 300 K, since the carrier density is temperature independent. Thus one should multiply the RRR value of graphite by a factor of 3 (i.e., $N_{300\,K}/N_{4.2\,K}$) in making comparisons to GIC's.

The Wiedemann-Franz law should apply to the analysis of the low-temperature thermal-conductivity measurements, since in the residual resistivity range, scattering is entirely due to static defects and is thus elastic. Here the electrical resistivity (identified with the residual resistivity ρ_r) is constant, corresponding to a linear T^1 dependence of the electronic thermal conductivity. It has been previously checked on a stage-4 $FeCl_3$ GIC that ρ was indeed constant in the range $T<10$ K, where the thermal conductivity varies linearly with temperature.[2]

Applying the Wiedemann-Franz relation [Eq. (3)] with a free-electron Lorenz number L_0 to the low-temperature linear part of the thermal conductivity, we have computed the low-temperature electrical resistivity ρ for the various stage $FeCl_3$ compounds investigated in the present work; the results are shown by the triangular points in Fig. 3. We see from this figure that the variation of ρ_r with reciprocal stage ($1/n$) follows the same type of dependence as is observed by direct measurement in inter-

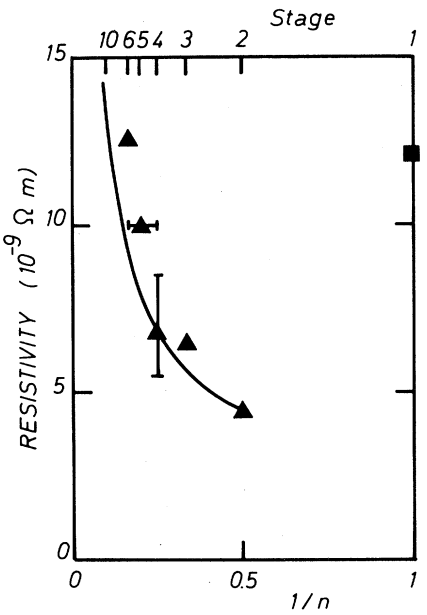

FIG. 3. In-plane residual resistivity ρ_r of graphite-$FeCl_3$ intercalation compounds as a function of reciprocal stage. The residual resistivity was calculated by applying the Wiedemann-Franz relation to the low-temperature linear part of the electronic thermal conductivity. The horizontal error bar is for the data obtained on the 4* mixed-stage compound. The data for a pure stage-4 are taken from Ref. 2 and the vertical uncertainty bar is mainly attributed to the uncertainty in the estimation of the distance between the thermometers on the small sample that was investigated in that work. All the dark triangles refer to our data while the dark square point for the stage-1 compound is taken from Ref. 15. The solid line is the calculated stage dependence using Eq. (7). (See text).

calation compounds around room temperature, where such data are available.[1] This suggests that in the residual range, it is mainly the change in carrier density with stage, and not a variation in the electron–static-defect interactions from one sample to another, which mainly governs the stage dependence of the resistivity in these compounds. It is thus implied that in our $FeCl_3$ GIC samples the defects introduced by intercalation do not vary significantly from one sample to another of the same stage or for compounds of different stages. It will be seen in Sec. IV B that this assumption also leads to consistent results when applied to lattice conduction and phonon-defect scattering near room temperature. It is worth noting that these assumptions are also in qualitative agreement with recent x-ray structural studies on two GIC's.[21,22] On the other hand, the assumption that the electron–static-defect interactions are stage independent is only assumed for the present set of graphite-$FeCl_3$ samples, which were prepared in the same way and from the same piece of HOPG. This assumption may not be applicable to other sets of GIC samples or to a stage-1 graphite-$FeCl_3$ sample. No stage-1 compounds were studied in the present work.

In our analysis of the in-plane residual resistivities of the $FeCl_3$ compounds we make use of the simple phenomenological picture recently proposed for the electrical conductivity[1,23] of compounds with stages $n \geq 2$:

$$\sigma_n = [d_i\sigma_i + 2c_0\sigma_{gb} + (n-2)c_0\sigma_{gi}]/I_c \ , \qquad (5)$$

where σ_n is the electrical conductivity of a sample of stage n, and σ_i, σ_{gb}, and σ_{gi} are, respectively, the conductivities of the intercalate, graphite bounding, and graphite interior layers (see Fig. 4). The c-axis repeat distance in Eq. (5) and Fig. 4 is

$$I_c = d_i + nc_0 \ , \qquad (6)$$

where d_i is the thickness of the intercalate layer and has the value 6.06 Å for $FeCl_3$ and 2.05 Å for potassium, and $c_0 = 3.35$ Å is the thickness of the carbon layers. There is a slight variation of the thickness of these layers according to the stage,[1,24,25] but this effect is too small to be of importance in the present discussion. Though naive, the two-dimensional model represented by Eq. (5) is plausible because of the high in-plane conductivity and low c-axis conductivity in these materials.

The electrical conductivity of the intercalant layer σ_i can usually be neglected[1,23] and we shall to a first approximation also neglect that of the graphite interior layers, because the carrier concentration in the graphite bounding layers far exceeds that in the interior layers. Thus Eq. (5) can be approximately written as

$$\rho_n = (d_i + nc_0)\rho_{gb}/2c_0 \ , \qquad (7)$$

where ρ_{gb} and ρ_n are the electrical resistivities of the graphite bounding layers and of the sample of stage n, respectively. In the simplest approximation, we assume that ρ_{gb} is independent of stage for $n \geq 2$.

From the value of the residual resistivity obtained for the $FeCl_3$ stage-2 compound,[26] $\rho_2 = 0.445 \times 10^{-8}$ Ω m, we may estimate ρ_{gb} for the bounding layers and obtain $\rho_{gb} = 0.232 \times 10^{-8}$ Ω m. Then using Eq. (7), we can determine ρ_n for various stages. We see from Fig. 3 (solid line) that this procedure underestimates the value of the resistivity for the higher stages. The difference between the measured and calculated values for ρ_n is greater than the experimental uncertainty for the measured thermal conductivity (Sec. II B).

At higher temperatures, the electronic thermal conductivity of the $FeCl_3$ compounds is more difficult to estimate for several reasons. First, except for the stage-1 compound[15] there are no available data for direct measurement of the temperature dependence of the resistivity. Second, even at room temperature where such data have been reported,[27] these data are too scattered to allow any quantitative analysis to be made of the stage dependence of the electrical resistivity. Third, it is likely that there is a narrow temperature region between liquid-helium and room temperature where the scattering is not elastic and the Wiedemann-Franz

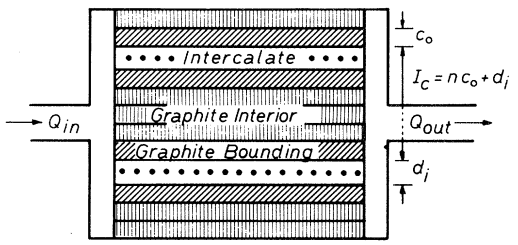

FIG. 4. Simple model for the in-plane electrical conductivity of GIC's (Ref. 23), which distinguishes between the intercalant nonconducting layer of thickness d_i, the highly conductive graphite bounding layers, and the less conductive graphite interior layers of thickness c_0. I_c is the c-axis repeat distance and n the stage of the compound. The same model is applied for the electronic thermal conductivity and for the lattice thermal conductivity where Q indicates the heat flux. However, in the case of lattice thermal conductivity no distinction is made between graphite interior layers and graphite bounding layers in the present work.

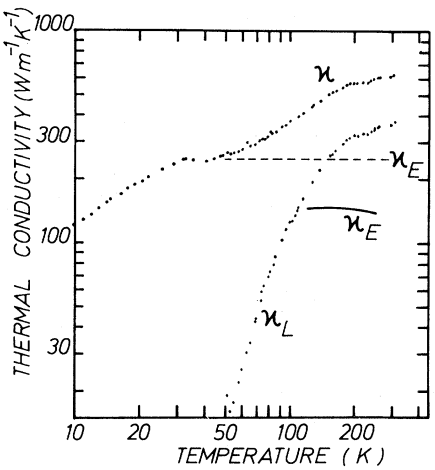

FIG. 5. Tentative separation of the electronic (κ_E) and lattice (κ_L) contributions to the in-plane thermal conductivity (κ_a) of a stage-5 graphite potassium intercalation compound. The upper points are relative to the measured total thermal conductivity, which is assumed to coincide with the electronic thermal conductivity κ_E in the low-temperature range and up to the onset of the plateau. The dashed line is the extrapolation to higher temperatures of the plateau of the electronic thermal conductivity. Subtraction of κ_E from κ [Eq. (1)] yields the lattice thermal conductivity κ_L (lower points). Note that in the lower-temperature range the uncertainty in κ_L is very large, since it results from the subtraction of two large numbers, and the exact ordinate of the plateau is difficult to locate accurately. The solid curve is the electronic thermal conductivity computed from the electrical resistivity data of McRae *et al.* (Ref. 28).

relation does not hold.

The situation is easier to analyze in the case of the K compound. It is evident from Fig. 1 that the electronic thermal conductivity is much higher at low temperature for this compound than for the $FeCl_3$ compounds and the electronic contribution is probably the dominant one up to about 45 K. This observation supports a higher charge transfer to the graphite in the case of the K intercalant as compared with $FeCl_3$. Also, below 10 K, the thermal conductivity varies linearly with temperature. Above 50 K, if we exclude the small features attributed to phase transitions, the electrical resistivity of the stage-5 K compound varies almost linearly with temperature.[17] This indicates that the electron scattering is dominated by large-angle electron-phonon scattering, a quasielastic process; thus the Wiedemann-Franz law should hold, and the electronic thermal conductivity should be temperature independent [Eq. (3)], as observed (see Figs. 1 and 5). Further, this behavior was experimentally observed on a stage-7 potassium compound with an electronic thermal conductivity varying linearly with temperature for $T<4$ K and a temperature-independent behavior above ~ 10 K.[6] Thus for our stage-5 potassium compound, a tentative way to separate the electronic and lattice contributions is to attribute the plateau of the thermal conductivity observed for the K sample in the narrow temperature range $30<T<45$ K to the onset of the "high-temperature" saturation behavior of the electronic thermal conductivity. With this identification, the relative contributions in Fig. 5 are obtained for the lattice κ_L (given by the points) and for the electrons κ_E (given by the dashed line). If, using the Wiedemann-Franz law, we compute the electronic thermal conductivities from the electrical resistivity data of McRae *et al.*[28] we obtain about half the magnitude (solid line in Fig. 5) of those deduced from our analysis. However, if we extrapolate to stage 5 the electrical resistivity measurements of Onn *et al.*[29] on stages 2, 3, and 4, we find that the corresponding κ_E data fall midway between our data and those computed from the measurements of McRae *et al.*[28] Because of the variation in residual resistivity from one sample to another of the same intercalant and stage, we consider the agreement between our analysis and the work of others to be satisfactory.

B. The in-plane lattice thermal conductivity

In this section, we shall first discuss the temperature dependence of the lattice thermal conductivity of the potassium compound, followed by a brief discussion of the stage dependence of the lattice thermal conductivity of the acceptor compounds.

The temperature variation of the lattice contribution κ_L is obtained upon subtraction of the electronic component κ_E from the measured value of the total thermal conductivity κ according to Eq. (1). The lattice contribution κ_L for the stage-5 potassium compound is presented by points in Fig. 5. The validity of this approach has been established experimentally for $T\leq 50$ K.[6] In the present discussion, we mainly focus on the higher-temperature range ($T>100$ K) where the lattice contribution dominates.

We see, by comparing Figs. 1 and 5, that the behavior of the lattice component of κ for the potassium stage-5 compound follows qualitatively that of pristine graphite. As the defect concentration increases, the peak in κ_L decreases in amplitude, broadens, and shifts to higher temperature,[7] con-

sistent with observations on these GIC's. The dip in the curve for κ_L around 200 K, where an anomaly was also observed in the thermopower,[4] is identified with a phase transition in the intercalate layer. This phase transition has been observed by many experimental techniques,[1] including anomalies in the electrical resistivity.[17,28,29] The temperature region around 200 K was carefully measured and the observed dip in κ_L is larger than the experimental uncertainty. Independent differential thermal analysis measurements that we performed in the range $150 < T < 300$ K confirmed the presence of a phase transition in our sample at ~ 230 K.

In modeling the thermal conductivity of intercalated graphite we note that the most important contribution above ~ 50 K comes from phonons associated with the graphite planes. As a first approximation we model this contribution on the basis of previous theories developed for the thermal conductivity of pristine graphite.

Many groups have dealt with the low-temperature thermal conductivity of pristine graphite.[30–36] Dreyfus and Maynard[32] and Kelly[33,34] have considered the influence of defects such as introduced by neutron irradiation or grain boundaries, while Kelly[33,34] and Hooker *et al.*[36] also considered the contribution of out-of-plane phonons and their scattering by defects along the c axis. Dreyfus and Maynard[32] confined themselves to a two-dimensional model. In the present work, we have experimental information for κ_L only in the temperature range $50 < T < 300$ K. In this region the two-dimensional model is adequate because of the low cutoff energy of the out-of-plane phonons.[37]

Before analyzing quantitatively the temperature variation of the lattice contribution in intercalated graphite, let us first try to identify the scattering mechanism that could be responsible for the reduction of the lattice thermal conductivity relative to pristine graphite. In graphite we are still in the low-temperature regime at room temperature with regard to the in-plane thermal properties. The Debye temperature for in-plane phonons in pristine graphite is very high ($\Theta_D \sim 2500$ K), and even though intercalating potassium into graphite reduces the mean Debye temperature,[38,39] Θ_D is still very large compared to values in common materials. Therefore, the upshift we observe in the temperature of the dielectric maximum T_m in the intercalated sample relative to pristine graphite could not be attributed to a variation of the Debye temperature, which would be expected to result in a small *decrease* in T_m with intercalation. Thus the shift of T_m to higher temperature after intercalation, as well as the decrease of κ_a at and below T_m, is consistent with the reduction of the phonon mean free path λ.

The temperature dependence of the lattice thermal conductivity of pristine graphite below T_m reflects that of the lattice specific heat C_v in a scattering regime where λ is temperature independent [Eq. (2)]. In pristine HOPG the dominant in-plane phonon scattering mechanism is phonon scattering at grain boundaries. In intercalated graphite, the magnitudes of the lattice thermal conductivities near and below T_m (compare Figs. 1 and 5) enable us to estimate that λ must be roughly an order of magnitude smaller than in HOPG.

Since in-plane phonon diffusion is two dimensional, a linear defect in the plane of phonon propagation will be as effective a scatterer as a surface defect in three-dimensional solids. We attribute the reduction of λ in the intercalated samples to the lattice distortions associated with large-scale defects introduced during the intercalation process. Such defects might arise from the bending of the graphitic layers in the vicinity of the previously proposed Daumas-Hérold domain boundaries,[40] where an acoustic mismatch is expected. This mismatch will cause a reflection of phonons, as occurs at grain boundaries in three-dimensional solids. On the other hand, our thermal-conductivity measurements are not sensitive to the detailed nature of the large-scale defects.

Below room temperature we are in the low-temperature regime with regard to the phonon scattering processes, and the relaxation time of phonons will be mainly determined by that of phonon-phonon interactions, phonon—point-defect scattering, and, below T_m, by that of phonon—large-scale-defect scattering. Low-energy phonons are dominant over the entire temperature range of the experiments. In the analysis, it is necessary to consider both normal processes and umklapp processes.

The relaxation frequency for phonon scattering by defects of much larger size than the phonon wavelength, such as boundaries, is given by

$$\tau_B^{-1} = v/\lambda_B \ , \tag{8}$$

where the boundary scattering length λ_B is within a numerical factor, usually small, equal to the distance between such defects, and τ_B^{-1} is independent of the phonon frequency ω. Point defects are those with a small size compared to the phonon wavelength, and their scattering frequency for two-dimensional solids has a functional dependence of[32]

$$\tau_D^{-1}=A\omega^3 . \tag{9}$$

While boundary and point-defect scattering are both resistive processes, we must distinguish between umklapp and normal processes in the discussion of phonon-phonon scattering. In the first case, the phonon-phonon interaction leads to a resistance to the thermal flow characterized by a relaxation frequency,

$$\tau_U^{-1}=Ux^{\alpha}T^{2\alpha}\exp(-\Theta_D/U_DT) , \tag{10}$$

where Θ_D is the in-plane Debye temperature, $x=\hbar\omega/k_BT$, α is a constant of the order of 2, U is a coupling parameter, and U_D a parameter with a numerical value between 2 and 3.[7] The parameters α, U, and U_D are determined by fitting Eq. (10) to experimental values of τ_U^{-1}.

Normal processes do not contribute directly to the thermal resistance, although they have an indirect influence since normal processes lead to the creation of higher-frequency phonons, which are more apt to undergo resistive processes. The relaxation frequency for such normal processes in a two-dimensional hexagonal solid is given by[32]

$$\tau_N^{-1}=N\omega T^3 , \tag{11}$$

where N is a coupling constant.

The total relaxation frequency τ_R^{-1} for all resistive processes is then

$$\tau_R^{-1}=\tau_U^{-1}+\tau_B^{-1}+\tau_D^{-1} . \tag{12}$$

We shall further define a relaxation frequency τ_c^{-1} which takes into account resistive as well as normal processes in such a way that

$$\tau_c^{-1}=\tau_N^{-1}+\tau_R^{-1} . \tag{13}$$

In the Callaway treatment of thermal conductivity[41] the total lattice conductivity κ_L is expressed as the sum of two terms:

$$\kappa_L=\kappa_1+\kappa_2 . \tag{14}$$

The first term κ_1 considers all collisions (including normal processes) as resistive mechanisms,

$$\kappa_1=\kappa_0\int_0^{\omega_D}\tau_c(\omega)c(\omega)d\omega , \tag{15}$$

where κ_0 is a constant factor, $\omega_D=\Theta_D/T$, and $c(\omega)$ is the contribution to the specific heat of a phonon of frequency ω. The correction term κ_2 makes allowance for the fact that N processes do not contribute directly to the thermal resistance[41]:

$$\kappa_2=\kappa_0\frac{\left[\int_0^{\omega_D}(\tau_c/\tau_N)c(\omega)d\omega\right]^2}{\int_0^{\omega_D}[\tau_c/(\tau_N\tau_R)]c(\omega)d\omega} . \tag{16}$$

For two-dimensional solids and replacing $c(\omega)$ by the expression given by Klemens,[30] these integrals become

$$\kappa_1=\frac{k_B^3}{2\pi c_0}\left[\frac{T}{\hbar}\right]^2\int_0^{x_D}\tau_c\frac{x^3e^x}{(e^x-1)^2}dx , \tag{17}$$

and

$$\kappa_2=\frac{k_B^3}{2\pi c_0}\left[\frac{T}{\hbar}\right]^2\frac{\int_0^{x_D}\frac{\tau_c}{\tau_N}\frac{x^3e^x}{(e^x-1)^2}dx}{\int_0^{x_D}\frac{\tau_c}{\tau_N\tau_R}\frac{x^3e^x}{(e^x-1)^2}dx} , \tag{18}$$

TABLE I. Values of the various parameters determining phonon scattering processes in pristine and intercalated graphite. Only the parameters λ_B and A are fitted to the κ_L for the GIC. For the parameters U, α, U_D, and N, the values for pristine graphite are used.

Symbol	Units	HOPG	Values K stage 5	$FeCl_3$ stage 2	$FeCl_3$ stage 3	$FeCl_3$ stage 6
λ_B[a]	m	1.55×10^{-5}	3.03×10^{-7}	5.83×10^{-7}	6.23×10^{-7}	7.70×10^{-7}
U[b]	$\sec^{-1}K^{-2}$	766	766	766	766	766
α[c]		1.44	1.44	1.44	1.44	1.44
U_D[d]		4.74	4.74	4.74	4.74	4.74
N[e]	10^{-11} K^{-3}	1.63	1.63	1.63	1.63	1.63
A[g]	10^{-32} $\sec^2$	0.58	3.28	1.82	2.56	2.34

[a] λ_B is the boundary scattering length.
[b] U is the coupling constant in Eq. (10) for umklapp processes.
[c] α is the quantity defined by Eq. (10).
[d] U_D relates to the fraction of Θ_D at the temperature of the most probable interacting phonon [Eq. (10)].
[e] N is the coupling constant for a normal process given by Eq. (11).
[f] A is the point defect scattering coupling constant given by Eq. (9).

where $x_D = \Theta_D/T$. These equations are applicable when only two of the graphite in-plane phonon modes carry the heat. This is the case for $T \gg T_x$, where T_x is the temperature corresponding to the cutoff frequency of the out-of-plane graphite phonons,[32] which from the phonon dispersion relations for pristine graphite is $T_x \cong 25$ K.[37] For GIC's, the density of low-frequency phonon modes is greatly increased, thereby increasing the channel for low-temperature thermal conduction by phonons.[42]

In our analysis of κ_L for pristine graphite we determined the parameters λ_B, A, α, U, U_D, and N in Eqs. (9)—(11) so that Eqs. (8)—(19) would fit the experimental values of κ_L measured on pristine HOPG in the temperature range $40 < T < 300$ K. The Debye temperature was taken equal to 2500 K.[32] The values of the parameters thus obtained are given in Table I.

In our analysis of the lattice thermal conductivity for intercalated graphite, we use the simplest possible phenomenological model through which we consider the total lattice conductance per unit cell to be equal to the sum of the conductances of the constituent graphite and intercalate layers of this unit cell (see Fig. 4). The total lattice conductance for a stage-n sample is then given by

$$\kappa_L = (d_i \kappa_{Li} + n c_0 \kappa_{LC})/I_c \ , \tag{19}$$

where κ_{Li} is the lattice thermal conductivity of the intercalant and κ_{LC} is that of the graphite in the intercalation compound. This value for κ_{LC} is lower than that of pristine graphite, since the thermal conductivity of the graphite layers is reduced by the lattice defects introduced by intercalation. In the higher-temperature range ($T > 50$ K) where the lattice thermal conductivity of the graphite layers, even after intercalation, is much higher than that of the intercalant, one may approximately write for a stage-n compound,

$$\kappa_L = n c_0 \kappa_{LC}/I_c \ . \tag{20}$$

Equations (19) and (20) imply that we neglect any differentiation between bounding and interior graphite layers when we consider phonon properties, quite unlike what we did with the electronic properties (Sec. IV A).[23] By assuming both types of graphitic layers to have the same phonon mean free path, we neglect phonon-electron scattering in considering phonon transport. This hypothesis is generally accepted in three-dimensional solids when the number of free carriers is smaller than 10^{-2} per atom.[7] Furthermore, defect scattering is expected to be the dominant scattering mechanism. This defect mechanism is strongly suggested by the lattice-fringing micrographs of Thomas *et al.*,[43] implying a random distribution of large-scale imperfections throughout the crystal. Recent lattice-fringing micrographs on well-staged graphite-$SbCl_5$ based on a single-crystal host material, however, indicate that samples can be prepared with large defect-free regions ($\sim 100 \times 2000$ Å^2).[44]

Using Eq. (20), the same calculation of κ_L as that for pristine graphite was made for the stage-5 potassium-intercalated graphite sample. In this calculation, the pristine graphite values for the various parameters were used with the exception of λ_B and A [see Eqs. (8) and (9)], which we treated as adjustable parameters, since they depend on the defect structure of the graphite planes. The result of the fit is given in Table I. From Table I we see that a boundary scattering length of $\lambda_B = 15.5 \times 10^{-6}$ m is obtained for pristine HOPG, which is to be compared with a basal crystallite size of approximately 10^{-6} m.[45] Thus in pristine HOPG the boundary scattering length is 1 order of magnitude larger than the size of the crystallites. This situation is not unexpected since large differences were previously observed between boundary scattering lengths estimated from thermal conductivity measurements and crystallite sizes determined by other techniques such as x rays.[46–48] To estimate the effect of intercalation, we see from Table I that λ_B is reduced in the stage-5 potassium GIC by a factor of ~ 50. Here we find a value of ~ 3000 Å for λ_B, which is again roughly an order of magnitude higher than the distance between large-scale defects in these compounds. Indeed Rousseaux *et al.*[21] observed by means of x-ray measurements for a stage-1 potassium compound an in-plane correlation length $\mathscr{L}$ of 400 ± 20 Å, and also noted that $\mathscr{L}$ was not very sensitive to staging.[22] Thus we see that, if for both the pristine HOPG and the intercalated potassium compound λ_B is 1 order of magnitude higher than the corresponding in-plane correlation length $\mathscr{L}$, the ratio $\lambda_B/\mathscr{L}$ is of the same order for both materials.

We also note from Table I that $A = 3.28 \times 10^{-32}$ sec^2 for the stage-5 potassium GIC as compared to 0.583×10^{-32} sec^2 for pristine graphite, indicating that point defect scattering is more effective in the intercalated sample than in pristine graphite; this is consistent with the increase in the concentration of point defects upon intercalation.

There is a much larger uncertainty with regard to the electronic component for the $FeCl_3$ compounds at high temperatures than that for the potassium

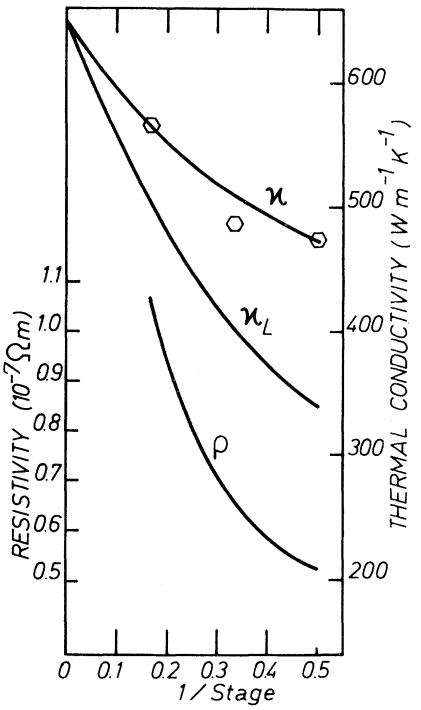

FIG. 6. Estimated stage dependence of the room-temperature ($T=290$ K) lattice thermal conductivity (right-hand scale) of graphite-$FeCl_3$ intercalation compounds obtained from the analysis given in the text. The hexagonal points represent the experimental values for the room-temperature in-plane thermal conductivity κ. The lower curve (left-hand scale) represents the stage dependence of the electrical resistivity ρ obtained from the electronic thermal conductivity $\kappa_E=\kappa-\kappa_L$ using the Wiedemann-Franz law (see text).

compounds. However, since we have experimental values for the total thermal conductivity for different stages, we may estimate qualitatively how both lattice and electronic contributions should vary with stage at a given temperature. To carry out this analysis, let us assume again that the lattice thermal conductivity of the graphite layers, whether bounding or interior layers, are the same.

The total thermal conductivity κ at room temperature is given by Eq. (1). Thus, if we know the stage dependence of the electrical conductivity at room temperature, we are able to deduce the lattice contribution κ_L from the experimental values of κ, if κ_E can be obtained from the measured stage dependence of the electrical resistivity ρ using the Wiedemann-Franz law. However, there is too much scatter in the data[27] available for the room-temperature stage dependence of ρ to make an accurate analysis in this way. Thus, to estimate the relative importance of κ_E and κ_L, we shall proceed in another way as outlined below.

For dilute stages, the electrical resistivity increases approximately linearly with stage index. Thus, in the limit of infinite stage, κ_E tends to a negligible small value, namely that for pristine graphite with defects; in this limit, the measured thermal conductivity is entirely due to the lattice contribution. In this analysis, we assume a stage dependence for κ_L given by Eq. (20) and a stage dependence of κ_E determined from Eq. (7) and the Wiedemann-Franz law. The magnitudes of κ_{LC} and σ_{gb} are, respectively, determined to be 650 $\mathrm{W\,m^{-1}\,K^{-1}}$ and $(27\pm3)\times10^{-9}$ Ω m by fitting to the measured values of κ for the stage-2 and -6 $FeCl_3$ GIC samples. The results thus obtained for the stage dependence of κ_L and ρ (obtained from κ_E) are presented in Fig. 6. Also included in the figure is a curve for the stage dependence of $\kappa=\kappa_L+\kappa_E$, which is constrained to pass through two points, as indicated above. The results obtained in Fig. 6 for the stage dependence of ρ are consistent with the direct room-temperature measurements of ρ by Perrachon *et al.*[27]

We may also roughly estimate the relative importance of the lattice and electronic thermal conduc-

TABLE II. Parameters governing the temperature dependence of the electrical resistivity of graphite-$FeCl_3$ intercalation compounds.

Stage of sample	ρ_r[a] (10^{-9} Ω m)	b[b] (10^{-9} Ω m)^2	$\rho_{290\,K}$[c] (10^{-9} Ω m)	a[d] (10^{-9} Ω m K^1)^2	RRR[e]
2	4.45	19.8	52.6	0.0327	11.8
3	6.40	41.0	66.3	0.0518	10.4
6	12.5	156.0	107.0	0.136	8.6

[a]ρ_r is determined from the low-temperature electronic thermal conductivity by applying the Wiedemann-Franz law [see Eq. (3) and Fig. 3].
[b]b is derived from Eq. (21) by assuming $T=0$ and $\rho=\rho_r$.
[c]The $\rho_{290\,K}$ values are taken from the analysis in Fig. 6.
[d]The a values are determined from Eq. (21) when $\rho=\rho_{290\,K}$ and $T=290$ K.
[e]RRR is the residual resistivity ratio.

tivities of the $FeCl_3$ compounds as a function of temperature. However, since we do not know the temperature variation of the electrical resistivity for compounds of higher stage, we must assume that, as for the stage-1 compound, all samples have a linear temperature dependence of the electrical resistivity above ~ 50 K. From the room-temperature values of ρ (denoted by $\rho_{290\,K}$) and from ρ_r (Table II), we then compute the temperature variation of ρ for each stage by means of an expression

$$\rho=(aT^2+b)^{1/2}\,, \tag{21}$$

which smoothly joins a temperature-independent region to a linear T regime. Values for a and b as determined from the resistivity values at 2 and 290 K are also given in Table II. Applying the Wiedemann-Franz relation, the temperature variation of the electronic contribution may then be computed and subtracted from the measured thermal conductivity to yield the lattice contribution. Although Eq. (21) may be a poor representation of the electrical resistivity, any error in it becomes a small error in κ_L because κ_E contributes no more than 25% of the total thermal conductivity near room temperature for any of the samples that were measured.

We may now estimate the importance of the lattice defects introduced by $FeCl_3$ intercalation in a similar way as we did for the stage-5 potassium GIC. These preliminary results are given in Table I. A more accurate analysis required a direct determination of the temperature dependence of the resistivity on the same samples. The large magnitudes (~ 6000 Å) of the large-scale defects in Table I are consistent with recent lattice-fringing results on a stage-2 graphite-$SbCl_5$ acceptor compound.[44] It is also seen from Table I that the boundary scattering length in $FeCl_3$ GIC increases as the stage increases, but this stage dependence is weak. This is consistent with the observation (Fig. 1) that the high-temperature flat maximum in the thermal conductivity occurs at temperatures which increase slightly with increasing stage. It also confirms that defects introduced by intercalation do not exhibit much stage dependence.

It may also be seen from Table I that point-defect scattering, though less important in $FeCl_3$ compounds than in the potassium stage-5 compound, is increased with respect to pristine graphite. The results also show that point defect scattering tends to increase slightly with increasing stage.

C. The c-axis thermal conductivity

The observed temperature dependence of the c-axis thermal conductivity is more difficult to interpret than the in-plane component, and this is so for several reasons. The results obtained in-plane can be extrapolated to the case of an ideal GIC single crystal, provided proper allowance is made for the quantitative differences in the scattering processes, mainly due to domain boundary scattering. For this reason the results for the temperature dependence of the in-plane thermal conductivity are believed to be of fundamental interest. This extrapolation is not so obvious for the case of the c-axis thermal conductivity.

Because of the large anisotropy in the thermal conductivity, one might while measuring the c-axis component measure at the same time a contribution from the in-plane component. This may occur for two reasons: (1) The c axes of the crystallites are not perfectly aligned but rather are oriented within a cone of 0.2° in pristine HOPG (Ref. 45) and this angle may be much larger for the intercalated materials. (2) If Daumas-Hérold domains exist, then graphitic layers which delineate these domains might carry the heat in the c-axis direction following a tortuous path.

A third reason that applies to the case of electrical conductivity measurements is not present for the thermal conductivity. In electrical conductivity measurements along the c axis, the sample edges may short-circuit the bulk when the proper precautions are not taken to avoid bending of the graphite planes around the edges.[49] However, in thermal-conductivity measurements, this problem does not seem to arise. At low temperature, this mechanism would give rise to a T^1 law in the c-axis thermal conductivity, which is not observed. If we analyze the curve for the c-axis thermal conductivity of the GIC in Fig. 2 as it stands, the magnitude of the thermal conductivity as well as the temperature dependence are similar to those of a heavily damaged dielectric.[7]

To verify further that the electronic contribution to κ_c is negligible, we compute the electronic thermal conductivity from the electrical resistivity[50] using the Wiedemann-Franz law. The results of this calculation show that the electronic contribution is between 4 and 5 orders of magnitude smaller than the measured thermal conductivity even at the lowest temperatures measured. This, as well as the behavior of the temperature dependence, indicates that lattice conduction is dominant over the whole temperature range, in contrast to the in-plane

thermal conductivity. A rough calculation, using approximate values for the specific heat and the measured value for the velocity of sound[51] in the c-axis direction, shows that if we use the Debye relation [Eq. (2)], the room-temperature mean free path of the phonons in the c-axis direction would be of the order of 10^{-10} m. This is smaller than the interatomic spacing and the dominant phonon wavelength at this temperature. Thus we face the same problem that was discussed in the case of the electrical conductivity of GIC's in this direction.[50] The small mean free path for the phonons raises a fundamental question as to the nature of the thermal conduction mechanism in this direction.

A quantitative model due to Kelly exists for the c-axis thermal conductivity in graphite.[34] It is, however, not possible to carry over Kelly's arguments directly to GIC's because the intercalate layers are effective scatterers for out-of-plane graphite phonons, which are expected to dominante c-axis thermal conductivity. Furthermore, in GIC's there is a much higher density of out-of-plane low-frequency phonon modes, and these modes have very low dispersion along k_z.[42]

V. CONCLUSIONS

In the present work we have analyzed the temperature and stage dependence of the in-plane thermal conductivity of acceptor graphite-$FeCl_3$ intercalation compounds. The temperature variation of the in-plane thermal conductivity of a donor graphite-K compound has also been analyzed, while preliminary results on the c-axis conductivity of a donor and an acceptor compound have been discussed.

The temperature dependence of the in-plane thermal conductivity of all samples measured so far confirms the trend inferred from preliminary investigations[2–5]: an increase in the electronic thermal conductivity of the graphite bounding layers in GIC's relative to pristine graphite and a decrease in the lattice thermal conductivity. The result is a thermal conductivity that for good samples is entirely electronic in the liquid-helium range and a mixture of lattice and electronic contributions at higher temperatures. We have also previously discussed the possible use of the electronic and lattice thermal conductivities as two independent tools to study the effect of intercalation[5] on electron and phonon scattering processes. The present work shows that this can be done. In particular, it is shown that the electronic thermal-conductivity contribution at low temperatures provides a powerful and independent tool for measuring the low-temperature in-plane electrical conductivity. Analysis of the present measurements shows that it is the variation in carrier density that most sensitively determines the stage dependence of the electrical conductivity of these compounds.

The results show that below room temperature the main scattering mechanism for phonons in the intercalated material is large-scale defects. The same situation occurs in pristine HOPG for temperatures below the dielectric maximum, where it is the size of the crystallites that determines the phonon mean free path. We have shown that the boundary length is about an order of magnitude larger than the crystallite size as was also previously observed. This boundary scattering length is also an order of magnitude higher in the stage-5 potassium compound than the in-plane correlation length observed on a stage-1 potassium compound. On the other hand, recent direct lattice-fringing results in single-crystal graphite-$SbCl_5$ indicated defect-free regions larger than 2000 Å.[44] It seems, however, difficult to come to definitive conclusions, since we are not comparing results of measurements performed on the same samples. Indeed, an interesting problem remaining to be solved is that of phonon-boundary scattering in two-dimensional solids. Parallel thermal-conductivity and electron microscopy or x-ray studies on the same intercalated material based on the same starting pristine HOPG material would be most useful to determine the relation between λ_B and $\mathscr{L}$.

Although electron scattering at low temperatures and phonon scattering below the dielectric maximum are not necessarily sensitive to the same static defects, the result of the analysis of the stage dependence of the low-temperature electronic thermal conductivity and that of the lattice thermal conductivity indicate that lattice defects are not strongly dependent on stage for $n \geq 2$. It should also be mentioned that the effect of the intercalant layer may be observed in a temperature range where the measured thermal conductivity is small.

The magnitude and temperature dependence of the c-axis thermal conductivity of GIC preclude any electronic contribution in this direction. Thus it is suggested that the phonons carry all the heat in the case of c-axis conduction. However, if analyzed in terms of the Debye theory, these phonons would have anomalously small mean free paths (less than a layer spacing) thus raising a fundamental question concerning the transport of heat in this direction. The present results, however, suggest an intrinsic conduction mechanism in the c direction since the

temperature dependence for κ_c is quite different from that for κ_a; nevertheless, the mechanism of basal plane short-circuiting by defects must also be considered. It is interesting to note also that at low temperatures we are in a unique situation where in the same sample the heat is carried by electrons in one direction and by phonons in the other direction. Finally, the anisotropy of the thermal conductivity is much smaller than that of the electrical conductivity and this explains *a posteriori* why it is possible to perform four-probe in-plane thermal conductivity measurements but not electrical resistivity measurements in acceptor GIC's.

The present analysis strongly suggests that the study of thermal-conduction phenomena in GIC's provides new insights into transport in two-dimensional systems generally.

ACKNOWLEDGMENTS

The portion of the work done at MIT was supported by the Air Force Office of Scientific Research (AFOSR Contract No. F49620-81-C-0006). The HOPG was kindly provided by Dr. Arthur W. Moore of Union Carbide. We are indebted to Dr. G. Dresselhaus, Dr. J.-P. Michenaud, and Professor F. J. Blatt for valuable comments during the course of the research. One of the authors (J.H.) acknowledges support from the Fonds National Belge de la Recherche Scientifique, and was a Visiting Scientist at the Francis Bitter National Magnet Laboratory, supported by the NSF, while part of this work was done. We also thank Mr. P. Coopmans for technical assistance with the experiments.

[1]M. S. Dresselhaus and G. Dresselhaus, Adv. Phys. 30, 139 (1981).

[2]J. Boxus, B. Poulaert, J.-P. Issi, H. Mazurek, and M. S. Dresselhaus, Solid State Commun. 38, 1117 (1981).

[3]B. Poulaert, J. Heremans, J.-P. Issi, I. Zabala-Martinez, H. Mazurek, and M. S. Dresselhaus, Extended Abstracts of the 15th Biennial Carbon Conference on Carbon, Philadelphia, 1981, edited by W. C. Forsman, p. 92.

[4]J. Heremans, J.-P. Issi, I. Zabala-Martinez, M. Shayegan, and M. S. Dresselhaus, Phys. Lett. 84A, 387 (1981).

[5]J.-P. Issi, J. Heremans, and M. S. Dresselhaus, in *Physics of Intercalation Compounds,* edited by L. Pietronero and E. Tosatti (Springer, Berlin, 1981), p. 310.

[6]J. Heremans, M. Shayegan, M. S. Dresselhaus, and J.-P. Issi, Phys. Rev. B 26, 3338 (1982).

[7]R. Berman, *Thermal Conduction in Solids* (Clarendon, Oxford, 1976).

[8]C. Underhill, S. Y. Leung, G. Dresselhaus, and M. S. Dresselhaus, Solid State Commun. 29, 769 (1979).

[9]M. Shayegan, M. S. Dresselhaus, and G. Dresselhaus, Phys. Rev. B 25, 4157 (1982).

[10]C. Underhill, T. Krapchev, and M. S. Dresselhaus, Synth. Met. 2, 47 (1980).

[11]G. K. White, in *Thermal Conductivity,* edited by R. P. Tye (Academic, London, 1969), p. 69.

[12]J.-P. Issi, J. Boxus, B. Poulaert, and J. Heremans, in Proceedings of the 17th Thermal Conductivity Conductivity Conference, Gaithersburg, Maryland, 1982, edited by J. Hust (Plenum, New York, in press).

[13]C. Zeller, A. Dennenstein, and G. M. T. Foley, Rev. Sci. Instrum. 50, 602 (1979).

[14]*Thermal Conductivity,* The TPRC data series, edited by Y. S. Touloukian (IFI/Plenum, New York, 1970). The data for κ_c in this reference should only by considered as a rough guide.

[15]L. A. Pendrys, T. C. Wu, C. Zeller, H. Fuzellier, and F. L. Vogel, Extended Abstracts of the 14th Biennial Conference on Carbon, State College, PA, 1979, edited by P. A. Thrower, p. 306.

[16]D. Guérard, G. M. T. Foley, M. Zanini, and J. E. Fischer, Nuovo Cimento 38B, 410 (1977).

[17]D. G. Onn, G. M. T. Foley, and J. E. Fischer, Phys. Rev. B 19, 6474 (1979).

[18]H. Suematsu, K. Higuchi, and S. Tanuma, J. Phys. Soc. Jpn. 48, 1541 (1980).

[19]I. L. Spain, in *Chemistry and Physics of Carbon,* edited by P. L. Walker (Dekker, New York, 1973), p. 1.

[20]Recent measurements of the temperature dependence of the electrical conductivity of intercalated benzene-derived fibers [T. C. Chieu, M. S. Dresselhaus, and M. Endo, Phys. Rev. B 26, 5867 (1982)] indicate that the residual-resistivity-ratio values are of comparable magnitudes ($\sim$6) for dilute donor alkali-metal–intercalated fibers and for acceptor-intercalated fibers.

[21]F. Rousseaux, A. Plançon, D. Tchoubar, D. Guérard, and P. Lagrange, in *Physics of Intercalation Compounds,* edited by L. Pieteronero and E. Tosatti, (Springer, Berlin, 1981), p. 228.

[22]D. Guérard and F. Rousseaux (private communication).

[23]M. S. Dresselhaus and S. Y. Leung, Extended Abstracts of the 14th Biennial Conference on Carbon, State College, PA, 1979, edited by P. A. Thrower, p. 496.

[24]R. Vangelisti and A. Hérold, Carbon 14, 333 (1976).

[25]A. Hérold, in *Physics and Chemistry of Materials with Layered Structures,* edited by F. Lévy (Dordrecht, Reidel, 1979), p. 323.

[26]A number of procedures could in fact have been used.

We could have chosen instead to calculate an average value for ρ_{gb} from the experimental values of ρ_n for the various stages measured and thus obtain an average value of $\rho_{gb}=(0.270\pm0.034)\times10^{-8}$ Ω m. With this value, ρ_n could be computed using Eq. (7) and another solid line would have been drawn in Fig. 3. However, these two procedures are equivalent for our purposes and yield curves that are within the accuracy of the measurements and analysis.

[27]J. B. Perrachon, C. Zeller, and F. L. Vogel, Extended Abstracts of the 14th Biennial Conference on Carbon, State College, PA, 1979, edited by P. A. Thrower, p. 304.

[28]E. McRae, D. Billaud, J. F. Mareche, and A. Herold, Physica 99B, 489 (1980).

[29]D. G. Onn, G. M. T. Foley, and J. E. Fischer, Mater. Sci. Eng. 31, 271 (1977).

[30]P. G. Klemens, Aust. J. Phys. 6, 405 (1953).

[31]J. E. Howe and A. W. Smith, Phys. Rev. 104, 892 (1956).

[32]B. Dreyfus and R. Maynard, J. Phys. (Paris) 28, 955 (1967).

[33]B. T. Kelly, Carbon 5, 247 (1967).

[34]B. T. Kelly, Carbon 6, 71 (1968).

[35]C. N. Hooker, A. R. Ubbelohde, and D. A. Young, Proc. R. Soc. London Ser. A 276, 83 (1963).

[36]C. N. Hooker, A. R. Ubbelohde, and D. A. Young, Proc. R. Soc. London Ser. A 284, 17 (1965).

[37]R. Al-Jishi and G. Dresselhaus, Phys. Rev. B 26, 4514 (1982).

[38]M. G. Alexander, D. P. Goshorn, D. G. Onn, D. L. Guérard, P. Lagrange, and M. El Makrini, Synth. Met. 2, 203 (1980).

[39]M. G. Alexander, D. P. Goshorn, and D. G. Onn, Phys. Rev. B 22, 4535 (1980).

[40]N. Daumas and A. Hérold, C. R. Acad. Sci. Ser. C 268, 373 (1969).

[41]J. Callaway, Phys. Rev. 113, 1046 (1959).

[42]R. Al-Jishi and G. Dresselhaus, Phys. Rev. B 26, 4523 (1982).

[43]J. M. Thomas, G. R. Millward, R. F. Schlögl, and H. P. Boehm, Mater. Res. Bull. 15, 671 (1980).

[44]G. Timp, M. S. Dresselhaus, L. Salamanca-Riba, A. Erbil, L. W. Hobbs, G. Dresselhaus, P. C. Eklund, and Y. Iye, Phys. Rev. B 26, 2323 (1982).

[45]A. W. Moore, in *Chemistry and Physics of Carbon,* edited by P. L. Walker and P. A. Thrower (Dekker, New York, 1973), Vol. 11, p. 69.

[46]B. T. Kelly and K. E. Gilchrist, Carbon 7, 355 (1979).

[47]B. T. Kelly, *Physics of Graphite* (Applied Science, London, 1981).

[48]A. de Combarieu, J. Phys. (Paris) 28, 951 (1967).

[49]D. Z. Tsang and M. S. Dresselhaus, Carbon 14, 43 (1976).

[50]J.-P. Issi, B. Poulaert, J. Heremans, and M. S. Dresselhaus, Solid State Commun. (in press).

[51]D. M. Hwang and B. F. O'Donnell, in *Physics of Intercalation Compounds,* Vol. 38 of *Springer Series in Solid State Sciences,* edited by L. Pietronero and E. Tosatti (Springer, Berlin, 1981), p. 193.